INTERNATIONAL JOURNAL OF PRECISION ENGINEERING AND MANUFACTURING Vol. 18, No. 7, pp. 915-922 JULY 2017 / 915

REGULAR PAPER

DOI: 10.1007/s12541-017-0108-2
ISSN 2234-7593 (Print) / 2005-4602 (Online)

Numerical Simulation of Chip Ploughing Volume in Micro Ball-End Mill Machining

Shan Luo[1], Abdolreza Bayesteh[1], Junghyuk Ko[1], Zuomin Dong[1], and Martin B. Jun[1,2,#]

1 Department of Mechanical Engineering, University of Victoria, Victoria, BC, V8W 2Y2, Canada
2 School of Mechanical Engineering, Purdue University, West Lafayette, IN, 47906, USA
Corresponding Author / E-mail: mbgjun@purdue.edu, TEL: +1-765-496-3376

KEYWORDS: Micro machining, Ball-end mill, Ploughing volume, Voxel, Cutting forces

Chip ploughing becomes a more serious problem in micro-machining due to its relatively large size with respect to the finished part, negatively impacting on the accuracy of the finished surface. In this work, a 3D geometry model of the chips generated during micro ball-end milling is introduced to accurately calculate the chip ploughing volume to support needed tool path adjustments for ensured accuracy of the finished part. A new method is developed to compute the chip ploughing volume by dividing the modeled chip into many discrete pieces over a ploughing dominated region and a shearing dominated region. Two simulation methods for calculating the chip volume for two example tool paths are presented. Different axial depths of cut, spindle speed and feed rate are tested to study the ploughing mechanism and reduce the ploughing effects. Experiments of cutting force measurement are used to compare with the changes of the simulated ploughing and shearing volume.

Manuscript received: August 22, 2015 / Revised: August 8, 2016 / Accepted: August 16, 2016

1. Introduction

With the advantages of higher accuracy and reduced costs, micro ball-end milling is able to produce various miniature components with complex geometry. Mechanical micro machining matters more to many industries than ever before from biomedical, electronics, automotive and aerospace applications.[1]

The ball-end milling process is widely used in machining dies and molds for automotive, medical and aerospace components with sculptured surfaces. Due to the constant radius between the cutter contact point and the center of the cutter, it is relatively easy to generate the tool path and to calculate the cutting forces and material remove rate (MRR) for a ball-end mill. However, whether these advantages would remain for micro ball-end milling process has not been well studied and understood. Certain macro cutting mechanisms are no longer applicable to micro milling any more due to the much smaller feed per tooth than the tool's cutting edge radius. The minimum chip thickness has not been considered in macro machining process. Furthermore, small micro tools lead to low cutter stiffness, elevated tool wear and breakage in machining a hardened workpiece with improper machining parameters.[2]

It is a challenging task to avoid ploughing problems in micro ball-end milling process due to the shapes of micro ball-end mills. When the cutter crosses the minimum chip thickness boundary, the tool would enter into the ploughing zone with no material removed. The uncut chip volume varies with the cutting edge and the depth of cut in the axial direction. The variation would result in the increase of ploughing area, which can cause increased thrust forces and chatter. It is vital to better understand the relations between ploughing, the depth of cut, feed rate, and the minimum chip thickness in the micro ball-end milling to improve the machining efficiency and surface quality.

A couple of studies have been conducted on the effects of minimum chip thickness and ploughing mechanisms with micro ball-end mills. Wang[3] analyzed the dual effects of shearing and ploughing mechanism in terms of axial depth of cut and tool radius through a set of slot machining tests. Yet the shearing and ploughing areas are constants due to the straight toolpath. Jun[4] reported that chip formation mechanism has changed in micro end milling, due to the change of relative size of the cutting edge radius to the chip thickness. The effects of minimum chip thickness and ploughing to cutting dynamics by a chip thickness model were investigated and the elastic recovery and elastic-plastic in the ploughing process was considered. However, the volume of an uncut chip has not been studied.

The first object of this work is to develop a new 3D chip model with a micro ball-end mill to accurately calculate the chip ploughing volume. The second goal is to reduce the ploughing effects. To better understand

the chip ploughing behavior under different cutting conditions and to obtain a generic solution to reduce the ploughing effect, different axial depth of cut and feed rates are tested to control the ploughing area. Tool paths are generated to simulate the machining process and get the relation between chip ploughing volume and cutting forces.

2. Ploughing Volume Prediction in Micro Ball-End Milling

2.1 Chip geometry modeling

Lim et al.[5] presented a 2D chip model to analyze the chip engagement surface and calculate the undeformed radial chip thickness with a ball-end mill. This model was further extended to a new 3D geometry model related the rank angle, shear plane area, chip thickness by Tsai et al.[6] An extended 3D chip geometry model with ploughing and shearing area has been developed as shown in Fig. 1. The slice plane is along the radial plane rather than the horizontal direction. The study on chip geometry involves the undeformed radial chip thickness in the cutting plane, the rotation angle, the inclination angle, and the surface generated by previous tooth path and the present machined surface. In order to calculate the chip volume in micro ball-end milling, a single horizontal cut with an axial depth of cut equal to the cutter radius has been proposed.

2.2 Ploughing volume calculation

In Fig. 1, the chip is divided into many slices along the radial direction. When the inclination angle θ is 90º, we can get the projection of the chip as shown in Fig. 2. Each layer of the chip has a shearing dominated area and a ploughing dominated area. As the chip thickness is less than minimum chip thickness, the tool is in ploughing area. In Fig. 2, O_1E is the radius of the cutter, denoted by R. OO_1 is the feed per tooth f_t, which can be obtained from:

$$f_t = \frac{f}{RPM \times N} \tag{1}$$

where, f is the feed rate in mm/sec. N is the number of flutes. OE is denoted by $r(\theta(i, j, k))$. The immersion angle at rotational angle θ_i for flute j and the k^{th} slice element $\theta(i, j, k)$ is measured by clockwise from y-axis. We can get the unknown side from two given length of sides and the angle between the two known sides:

$$R^2 = f_t^2 + r^2(\theta(i,j,k)) + 2r(\theta(i,j,k))f_t \sin(\theta(i,j,k)) \tag{2}$$

In Fig. 2, EF or t_c is the undeformed radial chip thickness. From the geometry, it can be known that

$$t_c(\theta(i,j,k)) = R - r(\theta(i,j,k)) \tag{3}$$

In the slice plane, the chip thickness is related to the inclination angle θ,

$$t_c(\theta(i,j,k),\phi) = t_c(\theta(i,j,k))\cos\phi \tag{4}$$

Substitute Eqs. (2) to (4), we can get:

$$t_c(\theta(i,j,k),\phi) = (R - \sqrt{R^2 + f_t^2 \sin^2\theta(i,j,k) - f_t^2} + f_t \sin\theta(i,j,k))\cos\phi \tag{5}$$

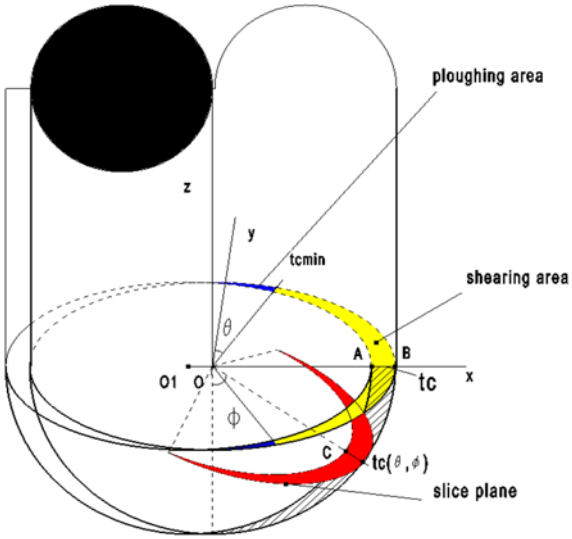

Fig. 1 A 3D chip geometry of micro ball-end mill feed in horizontal direction

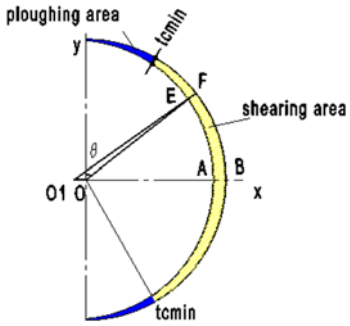

Fig. 2 The projection in the slice plane when the inclination angle θ is zero

Because of the helix flutes of micro ball-end mill, a point on the axis of the cutting edge will be lagging behind the end point of the tool. Thus, it requires considering the lag angle. If the helix angle on the tool is β, the new immersion angle should be:

$$\theta(i,j,k) = \theta_i + (j-1)\frac{2\pi}{N} - \frac{z(k)}{R}\tan\beta \tag{6}$$

where, N is the number of flutes, R is the radius of the k^{th} slice, $z(k)$ is the height of the k^{th} slice from bottom of the cutter, which can be determined as follows:

$$z(k) = R(1 - \cos(k - 0.5)\Delta\phi) \tag{7}$$

where, $\Delta\phi$ is the incremental inclination angle.

The chip model divides the chip into many small pieces of cuboid shape. When chip thickness $t_c(\theta, \phi)$ is less than minimum chip thickness t_{min}, the ploughing volume V_p for a tooth is calculated using the volume sum of the cuboids.

$$V_P = \sum \Delta A \times \Delta L = \sum_{\phi=0}^{\frac{\pi}{2}} \sum_{\theta=\theta_n}^{\theta_{ex}} t_c(\theta(i,j,k),\phi) \times R^2 \times \Delta\theta \times \Delta\phi \tag{8}$$

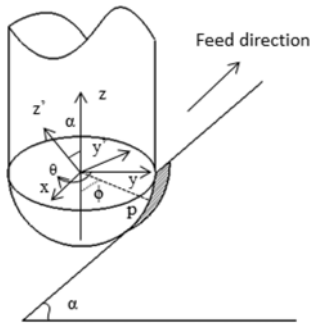

Fig. 3 Coordinate rotation for upward direction

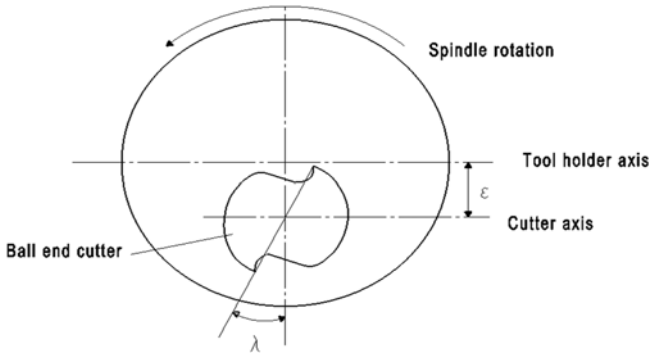

Fig. 4 Process faults with parallel offset runout

where, the entry and exit angles are $\theta_{st} = 0$ and $\theta_{ex} = \pi$ respectively, $\Delta\theta$ is the incremental rotation angle.

When the feed direction is not horizontal, but upwards as shown in Fig. 3, the chip geometry is different. The local coordinate system xyz is rotated by the x-axis, which makes y' axis parallel with the feed direction; z'-axis is perpendicular to the feed direction. In Fig. 3, from the geometry analysis, it can be known that the rotation angle α from z to z' is the inclination angle of the machining surface. P is a point on the cutting edge; its coordinate is expressed as following:

$$\begin{bmatrix} P_x \\ P_y \\ P_z \end{bmatrix} = \begin{bmatrix} R\cos\theta\cos\phi \\ R\sin\theta\sin\phi \\ -R\sin\phi \end{bmatrix} \tag{9}$$

The tool axis is rotated along x axis by an angle α. P in the local coordinate is transformed to P′ in the new coordinate as:

$$\begin{bmatrix} P_x' \\ P_y' \\ P_z' \end{bmatrix} = \begin{bmatrix} 1 & 0 & 0 \\ 0 & \cos\alpha & -\sin\alpha \\ 0 & \sin\alpha & \cos\alpha \end{bmatrix} \begin{bmatrix} R\cos\theta\cos\phi \\ R\sin\theta\sin\phi \\ -R\sin\phi \end{bmatrix} \tag{10}$$

In the $x'y'z'$ coordinate system shown in Fig. 3, assuming P' is:

$$P' = (R\cos\theta'\cos\phi', R\sin\theta'\sin\phi', -R\sin\phi') \tag{11}$$

From Eq. (10), we can calculate that

$$\begin{bmatrix} P_x' \\ P_y' \\ P_z' \end{bmatrix} = \begin{bmatrix} R\cos\theta\cos\phi \\ R\sin\theta\cos\phi\cos\alpha + R\sin\phi\sin\alpha \\ R\sin\theta\cos\phi\sin\alpha - R\sin\phi\cos\alpha \end{bmatrix} = \begin{bmatrix} R\cos\theta'\cos\phi' \\ R\sin\theta'\sin\phi' \\ -R\sin\phi' \end{bmatrix} \tag{12}$$

Therefore, θ' and ϕ' can be obtained from Eq. (12):

$$\begin{aligned} \phi' &= \sin^{-1}(\sin\theta\cos\phi\sin\alpha + \sin\phi\cos\alpha) \\ \theta' &= \cos^{-1}\left(\frac{\cos\theta\cos\phi}{\cos\phi'}\right) \end{aligned} \tag{13}$$

Then, the chip thickness t_c in Eq. (5) is modified as:

$$\begin{aligned} &t_c(\theta'(i,j,k), \phi') \\ &= (R - \sqrt{R^2 + f_t^2\sin^2\theta'(i,j,k) - f_t^2} + f_t\sin\theta'(i,j,k))\cos\phi' \end{aligned} \tag{14}$$

When the cutter moves upwards or downwards with a tilt angle, the chip thickness calculation is similar with the slot machining. The new immersion angle θ' and inclination angle ϕ' in Eq. (13) are obtained by the coordinate rotation.

2.3 Chip thickness calculation with runout

When process faults are considered, the radius of a particular tooth such as j^{th} tooth at the ith axial disk is $R(i, j)$ due to process faults. $R(i, j)$ is given by,[7]

$$R(i,j) = r(k) + \varepsilon\cos\left[z(k)\frac{\tan\beta}{R} - \lambda + (j-1)\frac{2\pi}{N}\right] \tag{16}$$

where, ε is the parallel offset runout, shown in Fig. 4; $r(k)$ is radius of the k^{th} slice, which can be determined as follows:

$$r(k) = R(1 - \sin(k - 0.5))\Delta\phi \tag{17}$$

$z(k)\tan\beta/R$ is the angle measured back from the tooth 1 to the j^{th} tooth, λ is the angle between the direction of the offset and the nearest tooth. λ is not easy to get, therefore in the paper, assuming λ is zero. $(j-1)2\pi/N$ is the angle measured back as the tooth engagement wraps up the helix.

The chip thickness with runout is:

$$t_{cnew} = t_c(\theta(i,j,k), \phi) + R(i,j) - R(i,j-1) \tag{18}$$

If $j = 1$, then

$$R(i,j-1) = R(i,N) \tag{19}$$

When the runout is larger than the feed per tooth, only the high side of the cutter would be cutting.[7]

2.4 Ploughing volume calculation algorithm

There are two methods for calculating the chip volume. One is based on the combination of Voxel and solid Boolean operation; the other is by getting the entry and exit angles from the Voxel method, and then having the volume integration along the sliced differential elements from the bottom of the tool toward the final axial depth of cut at each incremental rotation and inclination. Although both methods can calculate the chip volume, the first method cannot be used to obtain the ploughing volume due to its long calculation time and memory leak problem.

In this work, a two-step method is used for the calculation of the ploughing volume: a) calculate the reference immersion angle based on entry angle and exit angle for each cutting contact (CC) point; and b)

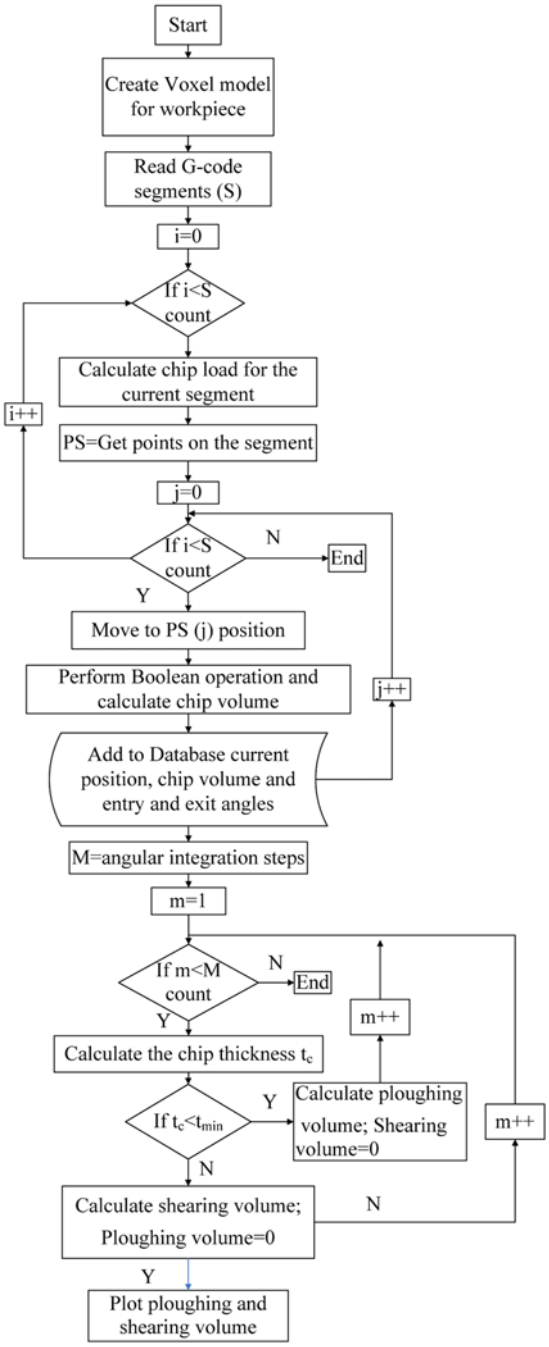

Fig. 5 The ploughing and shearing volume calculation flowchart

from the local view, calculate the ploughing volume and shearing volume according to the axial depth of cut, feed per tooth, start angle and end angle.

A general procedure of the ploughing volume simulation program is given in the flowchart as shown in Fig. 5. For step a), a Voxel model of the workpiece was created, and the input variables set by the user are workpiece width, height and thickness, chip thickness calculation scale factor, G-code program, axial depth of cut, the number of teeth, feed rate, spindle speed, and the cutter diameter.

The toolpath was divided into many segments, after input G-code, all of these segments were read and saved in the memory. Then, the tool was moved to the positions of cutter contact points and Boolean

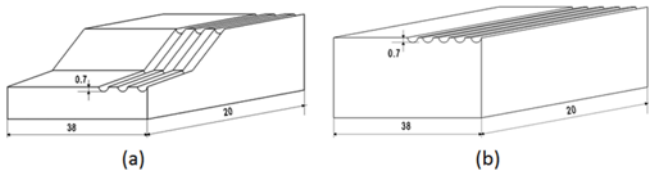

Fig. 6 Two different tool paths: (a) straight lines and down-ramping, (b) slot machining

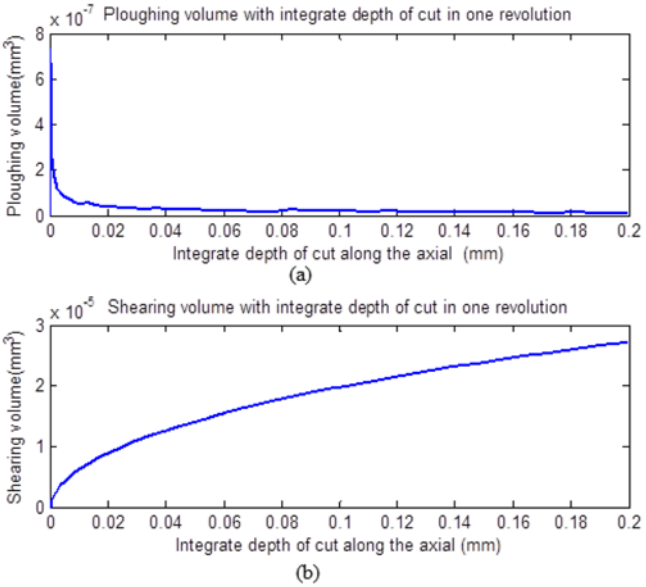

Fig. 7 (a) Ploughing volume changes with the integrate depth of cut in one revolution; (b) Shearing volume changes with the integrate depth of cut in one revolution

subtraction and intersection were used to calculate the chip total volume.[8] Finally, in the axial depth of cut plane, define a start point, connect the central point and the start point as the exit angle and then use the computational geometry method to find the largest angle to get the exit angle.

For step b), the depth of cut, feed per tooth, exit and entry angle, obtained in step a), and the helix angle are used to calculate the chip thickness. Present immersion angle is defined by exit and entry angle, when the present immersion angle is between zero and the reference immersion angle, the tool works and chips can be generated, otherwise, the cutting flute doesn't contact the workpiece. If the chip thickness is less than minimum chip thickness, calculate the ploughing volume, in this case, the shearing volume is zero. Vice versa, when the chip thickness is larger than minimum chip thickness, it just requires calculating the shearing volume.

3. Ploughing Volume Simulation

Two CNC tool paths were generated using MasterCAM to simulate the chip ploughing volume. The slot machining and the down-ramping and straight line machining can be seen in Fig. 6. The material of

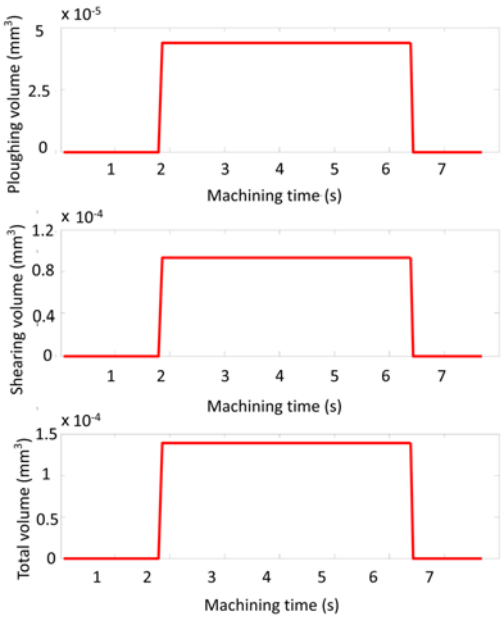

Fig. 8 Slot machining: chip volume simulations with machining times. Spindle speed = 20,000 rpm, depth of cut = 0.2 mm, f_t = 1 μm/tooth

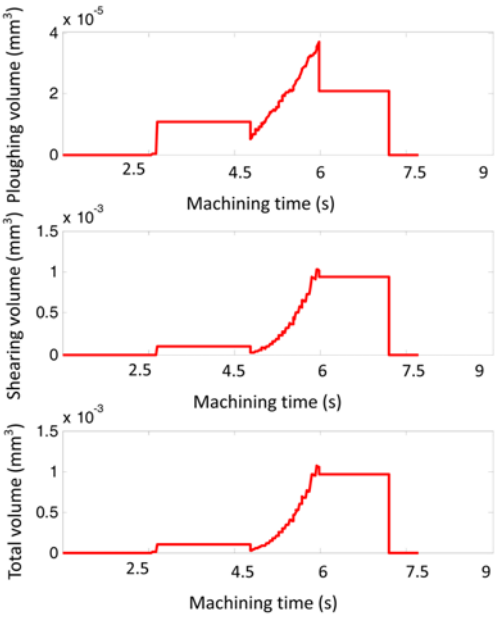

Fig. 9 Straight line and down-ramping machining: chip volume simulations with machining times. Spindle speed = 20,000 rpm, depth of cut = 0.2-0.7 mm, f_t = 1.5 μm/tooth

aluminum 6061 alloy, machined by tool diameter of 1/16" with two flutes micro ball-end mill is studied. The edge radius r_e of the tool is about 2 μm. The minimum chip thickness t_{min} for Al6061 aluminum is larger than $0.23r_e$.[9] In this paper, $0.3r_e$ is select-ed as the minimum chip thickness; the feed per tooth is 0.75 μm; and the depth of cut is 0.2 mm. For a slot machining, the relations between integrate depth of cut and ploughing and shearing volume are shown in Fig. 7. The simulation results show that as the depth of cut is decreased, the proportional ploughing volume increases as compared with the shearing volume.

The total chip volume was simulated by two different approaches: the Voxel combined with the Boolean method and the Voxel with integration method. For the first method, the chip volume was multiplied by a scale factor of 50 to reduce the number of subsegments of the toolpath and to save the calculation time. The second method can generate the same chip volume with the first method, and it can also calculate the shearing and ploughing volume.

For the toolpath of a straight line and down-ramping, two segments of the straight line still had a constant volume. For the down-cutting section, the total chip volume was supposed to have a linear increase. However, the depth of cut was varied. It was calculated by the positions of current and previous CC points in the Voxel and Boolean method. Some deviations exist in CAD model could cause errors in the Voxel and Boolean method. There are deviations when output the entry and exit angles from Voxel model. Therefore, some deviations exist in the Voxel and integration method and that is the reason why the chip volume for down-cut shown in Fig. 9 was not linear increased in the second method.

The phenomenon of ploughing leads to material deformation and side edges generation. It is important to investigate the ploughing volume and then predict cutting process to improve reliability and accuracy in machining. Figs. 8 and 9 show that ploughing volume is proportional

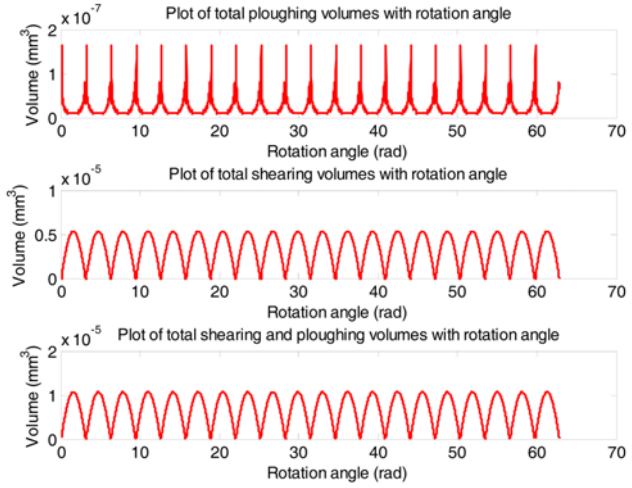

Fig. 10 Slot machining: chip volume simulations with rotation angle θ ignoring runout. Spindle speed = 40,000 rpm, depth of cut = 0.1 mm, f_t = 0.75 μm/tooth

to the shearing volume, and they have similar changes. It also indicates that high feed rate is helpful to reduce ploughing volume. Therefore, ploughing volume is significant to select optimal cutting parameters in micro-milling. The relation between chip volume and rotation angle θ in ten revolutions were illustrated in Figs. 10 and 11.

Eq. (16) shows that the radius of a particular tooth is relative to the Z axis of the tool rather than the rotation angle of the cutter. Therefore, as different teeth of the cutter are engaged in the machining, the rotation angle does not affect the run out on chip load.[7] When the parallel offset runout is considered, the ploughing and shearing volume is different at each flute cutting for a two-flute tool. It can be seen in Fig. 11, the

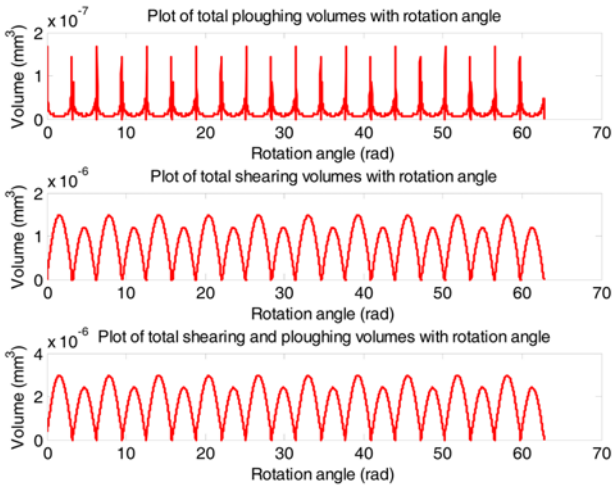

Fig. 11 Slot machining: chip volume simulations with rotation angle θ considering runout, ε = 0.01 μm, spindle speed = 40,000 rpm, depth of cut = 0.1 mm, f_t = 0.75 μm/tooth

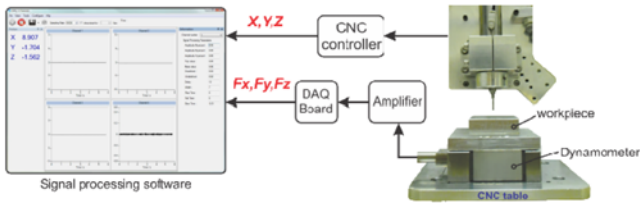

Fig. 12 Experimental setup of micro milling operations

shearing volume cut by a tooth is larger than that by the other tooth.

4. Experimental Setup

The verification experiments have been performed without lubricant (dry conditions) on a three-axis CNC ALIO vertical micro-milling machine. The range of the spindle speed of the machine is from 10,000 to 80,000 rpm. The experiment setup is shown in Fig. 12. A Kistler table dynamometer (MiniDyn 9256C1), connected with the feed table, was used to measure instant cutting forces. All of the instantaneous cutting forces are magnified by an amplifier and then displayed in a data acquisition (DAQ) board. The current position and cutting forces in three axes could be shown on the DAQ board.

In this experiment, a 1/16 two-flute ball end mill was used. The workpiece material is Aluminum 6061, and the workpiece size is 38 mm × 20 mm × 9 mm in length, width and height. Sampling rate or sampling frequency (*fs*) defines the number of samples per second. In the experiment, the sampling rate is 100 Hz, which is the upper band limit of the signal.

$$\text{Samples per interval} = \frac{\text{Sampling rate}}{RPM} \tag{20}$$

From Eq. (10), it can be known that if the spindle speed is 60,000 RPM, there are around 100 points for each revolution, when plot the

Table 1 The parameters for four group's experiments

Group number	Toolpath	Depth of cut (mm)	Spindle speed (rpm)	Feed per tooth (μm)
a	Straight line	0.1	40,000	0.75
b	Straight line	0.2	40,000	0.75
c	Straight line	0.2	40,000	2
d	Straight-down line	0.15-0.6	20,000	1.5
e	Straight-down line	0.2-0.7	20,000	1.5

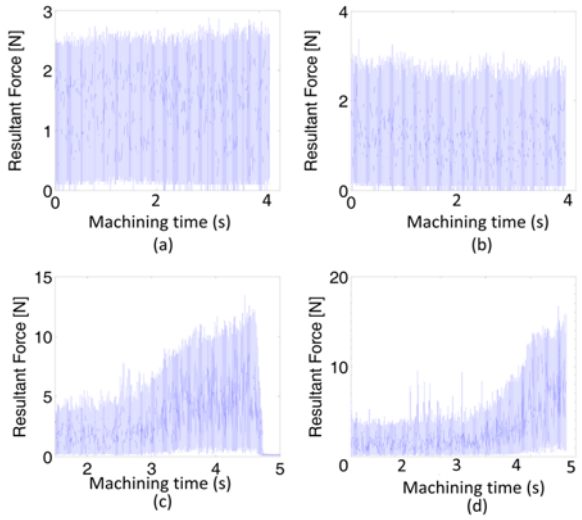

Fig. 13 Measured resultant cutting forces: (a) depth of cut d_c = 100 μm, f_t = 0.75 μm/tooth; (b) d_c = 200 μm, f_t = 0.75 μm/tooth; (c) d_c = 150-600 μm, f_t = 1.5 μm/tooth; (d) d_c = 200-700 μm, f_t = 1.5 μm/tooth

cutting forces. The resultant force is the sum of F_x, F_y, and F_z:

$$R = \sqrt{F_x^2 + F_y^2 + F_z^2} \tag{21}$$

Two different tool paths, shown in Fig. 6, were machined at different cutting parameters such as depth of cut, spindle speed, and feed rate. The experiments were divided into four groups shown in Table 1 with two different spindle speeds: 20,000 and 40,000 rpm, and two different feed rates: 0.75 and 1.5 μm/tooth. The depth of cut for the group a) and b) were constant: 0.1 and 0.2 mm respectively. The depth of cut was changed from 0.15 to 0.6 mm for group d) and from 0.2 to 0.7 mm for group d).

5. Experimental Results

Cutting force is the foundation to determine optimal cutting parameters. Chip volume calculation is easier than cutting force prediction. If the chip volume has similar changes with the cutting force, chip volume can also be used to select optimal cutting parameters. Fig. 13 shows the measured resultant cutting forces. The parameters setting were illustrated in Table 1. Compared the simulated total chip volume (shown in Fig. 10) and the experimental resultant cutting forces, their changes seem to be similar. When kinematics and certain properties

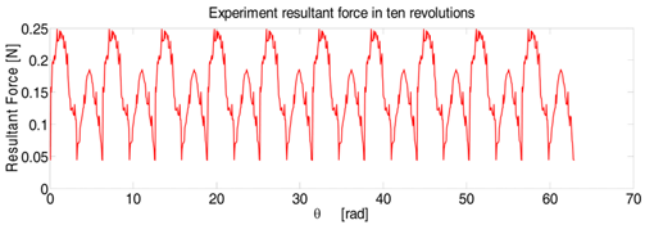

Fig. 14 Measured resultant cutting force for slot machining. Spindle speed = 40,000 rpm, depth of cut = 0.1 mm, f_t = 0.75 μm/tooth

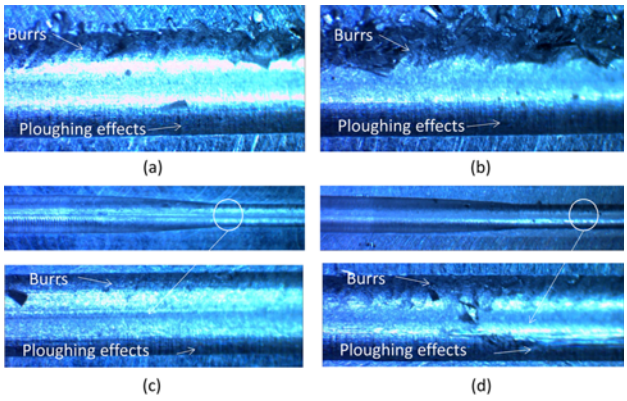

Fig. 15 The surfaces generated by ball-end milling: (a) depth of cut d_c = 100 μm, f_t = 0.75 μm/tooth; (b) d_c = 200 μm, f_t = 0.75 μm/tooth; (c) d_c = 150-600 μm, f_t = 1.5 μm/tooth; (d) d_c = 200-700 μm, f_t = 1.5 μm/tooth

of the milling process were considered, for the slot tests, the experiment data of the resultant cutting force were not constant due to vibration, but with some fluctuation in a reasonable range.

An accurate prediction of total chip volume for a micro-ball end mill is necessary to predict the cutting forces in process planning, studies of the interaction between tool and the milling process, and the errors left on the finish surface.

The ploughing and shearing volume depended on the rotation angle θ, the depth of cut. The differential ploughing and shearing volume are integrated along the in-cut portion of the tool from rotation and inclination directions to get the total chip volume generated by the flute.

Figs. 10 and 14 gave simulated chip volumes and the measured resultant cutting force for ten revolutions of the slot machining. It can be observed that the total chip volume shown in Fig. 10 is the absolute value of sinusoidal variation with the rotation angle. The simulation didn't consider the tool wear and vibrations. The shape of the curves of measured resultant force and simulated chip volume is similar. The mechanistic model also assumes that the ploughing forces are proportional to the ploughed volume of the material. However, Fig. 14 shows that the magnitudes of resultant cutting force between two flutes of the tool are different. That is due to one tooth has a more in-cut portion with the workpiece than the other and therefore more cutting force is generated. Compared Figs. 11 and 14, as the runout effects are considered, the shapes of shearing and total volume are similar with resultant force.

The surfaces generated by micro ball-end mill machining were

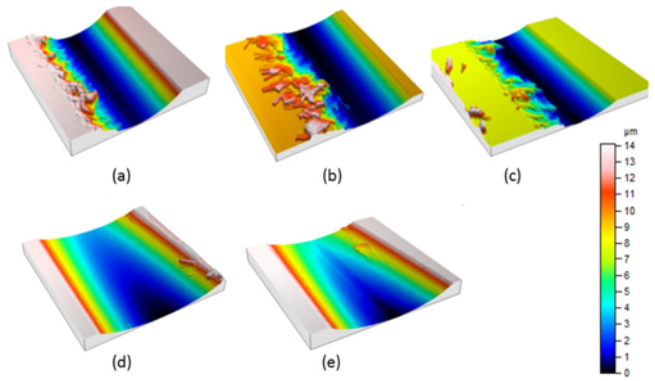

Fig. 16 Topography of machined surface in 3D surface measurement machine: (a) depth of cut d_c = 100 μm, f_t = 0.75 μm/tooth; (b) d_c = 200 μm, f_t = 0.75 μm/tooth; (c) d_c = 200 μm, f_t = 2 μm/tooth; (d) d_c = 150-600 μm, f_t = 1.5 μm/tooth; (e) d_c = 200-700 μm, f_t = 1.5 μm/tooth

inspected using a microscope. Ploughing is related to moderate wear, cutting process damping and tool stability. The ploughing effect happens when the flank face of the tool contacts the machined surface.[10] It leads to rough surface and burrs formation. A significant number of side burrs generation is associated with the heavy ploughing resulted from the large edges. Fig. 15(a) shows the surface produced by milling operations with a 100 μm depth of cut and feed rate of 0.75 μm per flute has fewer burrs and ploughing effects than the surface with the same feed rate but a larger depth of cut (shown in Fig. 15(b)). It demonstrates that the ploughing effect is subject to the depth of cut: a larger depth of cut is associated with a significant ploughing effect. Furthermore, at a high feed rate, the ploughing effects are less observable. Compared the surface results in Figs. 15(a) and (b) with that in Figs. 15(c) and (d), it can be seen that smaller depth of cut and higher spindle speed obtained better finish surface and fewer burrs happened. The parameters in Figs. 15(a) and (b) are from the group a) and b) in the Table1. The parameters in Figs. 15(c) and (d) are from the group d) and e) in the Table 1.

Overall, the ploughing phenomenon is expected to decrease as the feed rate is increased. In micro ball end milling, the ploughing effects are easier seen due to the tool geometry. The burrs are more significantly seen in one side of the machined surface. That is because the ploughing effects are more obvious at cutting entry than at exit.

The surface roughness is obtained by a 3D surface measurement machine. The surface quality of side wall in Fig. 16(c) is better than that in Fig. 16(b), due to the high feedrate. Compared the side walls with good surface quality, the ploughing effect of group c is less obvious than group b. When comparing Figs. 16(a) and (b), it can be known that the depth of cut also affects the side wall roughness. Larger depth of cut leads to higher surface roughness and poor surface quality.

6. Conclusions

A 3D geometry model and a discrete chip ploughing volume prediction method in micro ball-end milling were introduced in this work. Two CNC tool paths were used to simulate the machining process

and to obtain the relation between chip ploughing volume and cutting forces. The simulated chip volume has been qualitatively compared with measured cutting forces. The simulation results and cutting tests on Aluminum 6061 parts led to the following conclusions:

- As uncut chip thickness varies from thin to thick in one revolution, simulations results show high ploughing volume when uncut chip thickness is low.
- The resultant cutting force was seen to be proportional to the total chip volume of machined material.
- High feed rate can diminish ploughing volume and ploughing effects.
- The model can be used to predict ploughing volume for a complicated tool paths in micro ball-end milling.

ACKNOWLEDGEMENT

Financial supports from the Natural Sciences and Engineering Research Council of Canada, the Technology Innovation Program (100 53248, Development of Manufacturing System for CFRP (Carbon Fiber Reinforced Plastics) Machining) funded by the Ministry of Trade, industry & Energy (MOTIE, Korea) and the China Scholarship Council are gratefully acknowledged.

REFERENCES

1. Chen, M. J., Wang, Z. J., Wu, C. Y., and Ni, H. B., "Research on the Influence Factors for the Deflection of Micro-Ball-End Cutter in Micro-End-Milling Process," Materials Science Forum, Vols. 697-698, pp. 84-87, 2012.
2. Kim, C.-J., Bono, M., and Ni, J., "Experimental Analysis of Chip Formation in Micro-Milling," Transactions of NAMRI/SME, Vol. 30, pp. 1-8, 2002.
3. Wang, J.-J. and Zheng, C., "Identification of Shearing and Ploughing Cutting Constants from Average Forces in Ball-End Milling," International Journal of Machine Tools and Manufacture, Vol. 42, No. 6, pp. 695-705, 2002.
4. Jun, M. B. G., Liu, X., DeVor, R. E., and Kapoor, S. G., "Investigation of the Dynamics of Micro End Milling - Part I: Model Development," Journal of Manufacturing Science and Engineering, Vol. 128, No. 4, pp. 893-900, 2006.
5. Ee Meng, L., Feng, H.-Y., Menq, C.-H., and Lin, Z.-H., "The Prediction of Dimensional Error for Sculptured Surface Productions using the Ball-End Milling Process. Part 1: Chip Geometry Analysis and Cutting Force Prediction," International Journal of Machine Tools and Manufacture, Vol. 35, No. 8, pp. 1149-1169, 1995.
6. Tsai, C.-L. and Liao, Y.-S., "Prediction of Cutting Forces in Ball-End Milling by Means of Geometric Analysis," Journal of Materials Processing Technology, Vol. 205, No. 1, pp. 24-33, 2008.
7. Kline, W. A. and DeVor, R., "The Effect of Runout on Cutting Geometry and Forces in End Milling," International Journal of Machine Tool Design and Research, Vol. 23, Nos. 2-3, pp. 123-140, 1983.
8. Bayesteh, A. and Jun, M. B. G., "Feed Rate Optimization Issues in Micro-Milling," Proc. of NAMRI/SME, 2013.
9. Malekian, M., Mostofa, M. G., Park, S. S., and Jun, M. B. G., "Modeling of Minimum Uncut Chip Thickness in Micro Machining of Aluminum," Journal of Materials Processing Technology, Vol. 212, No. 3, pp. 553-559, 2012.
10. Paris, H., Brissaud, D., Gouskov, A., Guibert, N., and Rech, J., "Influence of the Ploughing Effect on the Dynamic Behaviour of the Self-Vibratory Drilling Head," CIRP Annals-Manufacturing Technology, Vol. 57, No. 1, pp. 385-388, 2008.